Laser-Induced Graphenization of PDMS as Flexible Electrode for Microsupercapacitors

ADVANCED MATERIALS INTERFACES
www.advmatinterfaces.de

Laser-Induced Graphenization of PDMS as Flexible Electrode for Microsupercapacitors

*Pietro Zaccagnini, Chiara Ballin, Marco Fontana, Matteo Parmeggiani, Stefano Bianco, Stefano Stassi, Alessandro Pedico, Sergio Ferrero, and Andrea Lamberti**

Laser graphenization of polymeric surfaces has emerged as one of the most promising technologies to fabricate flexible electrodes. Unfortunately, despite the large number of materials suitable for laser-induced graphene (LIG) fabrication, there is a lack of stretchable polymers, hindering the full exploitation of LIG for flexible electronics. Herein, the laser graphenization of polydimethylsiloxane (PDMS), the most exploited elastomeric substrate for flexible electronic device fabrication, is proposed for the first time. The low carbon content and the absence of aromatic structures strongly limit the graphenization process resulting in limited conduction properties. Nevertheless, by adding triethylene glycol (TEG) as carbon source into the PDMS matrix, it is possible to improve the graphenization and to reduce the sheet resistance of the written LIG by two orders of magnitude down to 130 ohm sq^{-1}. The PDMS-TEG material becomes a suitable candidate for flexible microsupercapacitor fabrication with specific capacitance values as high as 287 μF cm^{-2} and energy and power density approaching LIG-based supercapacitors fabricated onto traditional polyimide substrates.

1. Introduction

The future of portable electronics will surely be flexible. This is the key concept emerging from the last decade literature related to sensors, energy devices and antennas, i.e., the three main components of a portable electronic system.[1] Indeed the emerging field of Internet of Things needs hardware supports and not only data connection and analysis. Moreover, all of them must be conformable to curved and complex surfaces.[2] However, the way to reach the target of totally flexible devices is still long and full of obstacles that strongly obstruct the development of such systems.[3] Among the main limitations, it is possible to observe that there is an urgency of effective strategies to obtain conductive paths onto flexible substrates.[4] Moreover, even if the flexibility is mandatory, stretchable substrates are even more desired since the portable device sector is moving toward a wearable configuration. This implies that it is not possible to keep flexibility and stretchability separated.

In this context, laser induced graphene is emerging, in the large family of graphene-based materials,[5] as one of the most promising materials for the fabrication of flexible electronic devices.[6] However, despite the endless efforts spent to develop LIG on new substrates there is a lack of stretchable polymers suitable for laser graphenization.[7] Indeed, up to now the evidence of graphenization of elastomeric substrate has never been observed.

Considering the family of elastomer polymers, polydimethylsiloxane (PDMS) represents the most popular elastomeric material in microsystem technology thanks to its attractive physical and chemical properties such as elasticity, optical transparency down to 220 nm, tunable surface chemistry, low water permeability but high gas permeability and high dielectric properties. Moreover, it is a cost-effective material and allows the development of reliable mass replication technique.[8]

Unfortunately, it cannot be easily graphenized by direct laser writing because of the low amount of carbon linked to the siloxane chains, mainly consisting of methyl groups. For this reason, some research groups proposed the transfer of a LIG layer produced onto polyimide onto PDMS by simple infiltration of the uncured elastomer into the LIG network and subsequent peeling after the PDMS cross-linking.[9] This strategy allows to achieve stretchable electrodes, but strongly affects the conductivity of the transferred layer reducing its available surface area.[10] Moreover, the two-step process increases the fabrication time and complexity reducing the degrees of freedom during sample production.

We recently proposed an easy way to overcome the above-mentioned limitation by exploiting an innovative composite of polyimide microparticles dispersed into PDMS matrix.[11] The particles undergo a perfect graphenization during laser writing, but such procedure cannot solve all the problems previously discussed. In these composites the conductivity remains

P. Zaccagnini, C. Ballin, M. Fontana, M. Parmeggiani, S. Bianco, S. Stassi, A. Pedico, S. Ferrero, A. Lamberti
Politecnico di Torino
Dipartimento di Scienza Applicata e Tecnologia (DISAT)
Corso Duca Degli Abruzzi, 24, Torino 10129, Italy
E-mail: andrea.lamberti@polito.it

P. Zaccagnini, M. Fontana, M. Parmeggiani, A. Lamberti
Istituto Italiano di Tecnologia
Center for Sustainable Future Technologies
Via Livorno 60, Torino 10140, Italy

The ORCID identification number(s) for the author(s) of this article can be found under https://doi.org/10.1002/admi.202101046.

DOI: 10.1002/admi.202101046

limited by the connection among the LIG layer produced on the single particles which is much different with respect to an uninterrupted LIG film achievable onto a continuous polyimide surface.

Herein, after a careful tuning of the laser parameters, we demonstrate for the first time the graphenization of PDMS surface by CO_2 laser irradiation. The low carbon content and the missing aromatic structures still limit the graphenization process resulting in limited conduction properties. Nevertheless, by adding triethylene glycol (TEG) as carbon source into the PDMS matrix, it is possible to improve the graphenization degree and to reduce the sheet resistance of the written LIG on PDMS/TEG composite by two orders of magnitude down to 130 ohm sq^{-1}. The resulting material become a suitable candidate for flexible microsupercapacitor fabrication with specific capacitance values as high as 287 μF cm^{-2} and energy and power density approaching the LIG-based supercapacitors fabricated onto polyimide substrates.

2. Results and Discussion

Different laser parameters and multiple writing steps have been investigated in order to induce a graphene-like structure on PDMS and to increase as much as possible its conductivity. The optimization on laser parameters focuses on frequency (kHz), power (expressed in percentage with respect to the maximum value of 30 W), velocity (mm s^{-1}) and number of repetitions of writing path (see Supporting Information). The multiple laser technique was already described by Tour and co-workers and it allows enhancement of the electrical properties when no aromatic structure is present in the starting substrate.[7] As described in their paper the reason for this phenomenon relies on an intermediate conversion of the polymer into amorphous carbon and then into LIG. In Table S1 (Supporting Information) are listed the best parameters found in ambient conditions while Figure S1 (Supporting Information) collects the resulting sheet resistance values.

As it is possible to observe, all the parameters play an important role in the final electrical performance of the samples as previously discussed in other works.[11–13] However, the lowest sheet resistance achievable on bare PDMS surface remains quite high (650 ohm sq^{-1}) compared to the commonly obtained results on polyimide (about 20 ohm sq^{-1}).[13]

In order to increase the carbon content, we propose to add Triethylene glycol (TEG) during the PDMS mixture preparation.

The addition of TEG into PDMS allows to solve the graphenization problems observed on bare PDMS with the possibility to tune the LIG conductivity by simply varying the TEG percentage into the elastomer matrix. When TEG is inserted into the PDMS matrix, the resulting sample becomes opaquer than bare PDMS and tends to ivory (see **Figure 1**a). Figure 1b shows the reduction of the sheet resistance down to about 130 ohm sq^{-1} by adding up to 40% of TEG into PDMS. The 40% was found as the maximum amount of TEG that can be used without affecting the crosslinking of the elastomer. Indeed, by adding 50% of TEG the resulting materials have no sufficient mechanical stability to be removed from the mold.

However, we demonstrate that the mechanical properties of the composite are only slightly influenced by the addition of TEG in the concentration range 0%–40%. The Young's modulus of the bare PDMS samples is reduced from 1.64 to 1.34 MPa in the PDMS-TEG10% composite and further reduce to 1.02 MPa increasing the TEG concentration up to 40%. The reduction of Young's modulus with the addition of TEG was expected since this liquid component is normally used as plasticizer to decrease the plasticity or the viscosity of a polymer. Samples of the PDMS and PDMS-TEG composite with LIG lines written on the surface were also tested, and as expected no variations of the mechanical properties were observed.[11] The thickness of the material affected by the LIG formation process is much smaller with respect of the whole sample thickness (few tens of micrometers versus 1 mm) and it does not induce significant alteration of the macroscopic mechanical properties. The measured values are in line with standard Young's modulus range of PDMS from different producers.[14] Moreover, it is

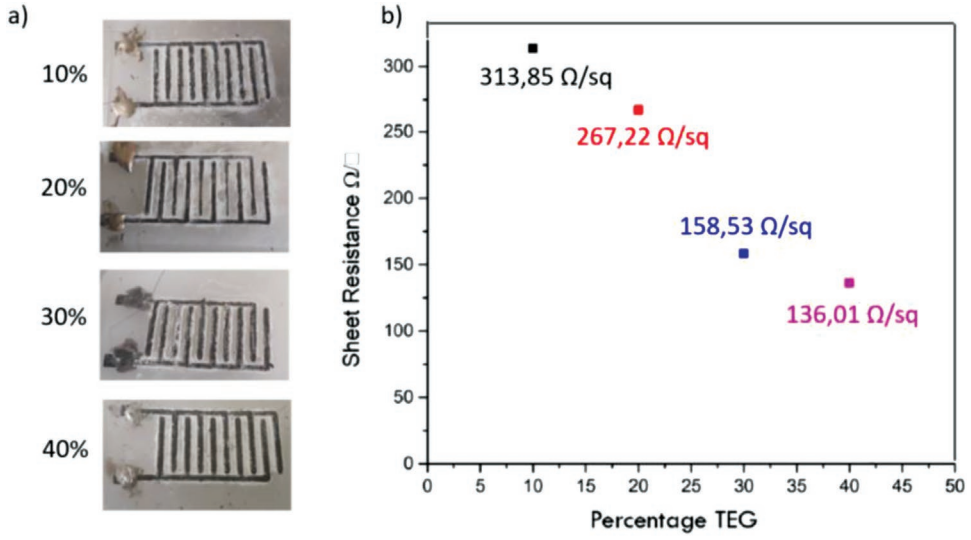

Figure 1. Digital photographs of the LIG written on the PDMS/TEG with different TEG percentage a) and respective sheet resistances b).

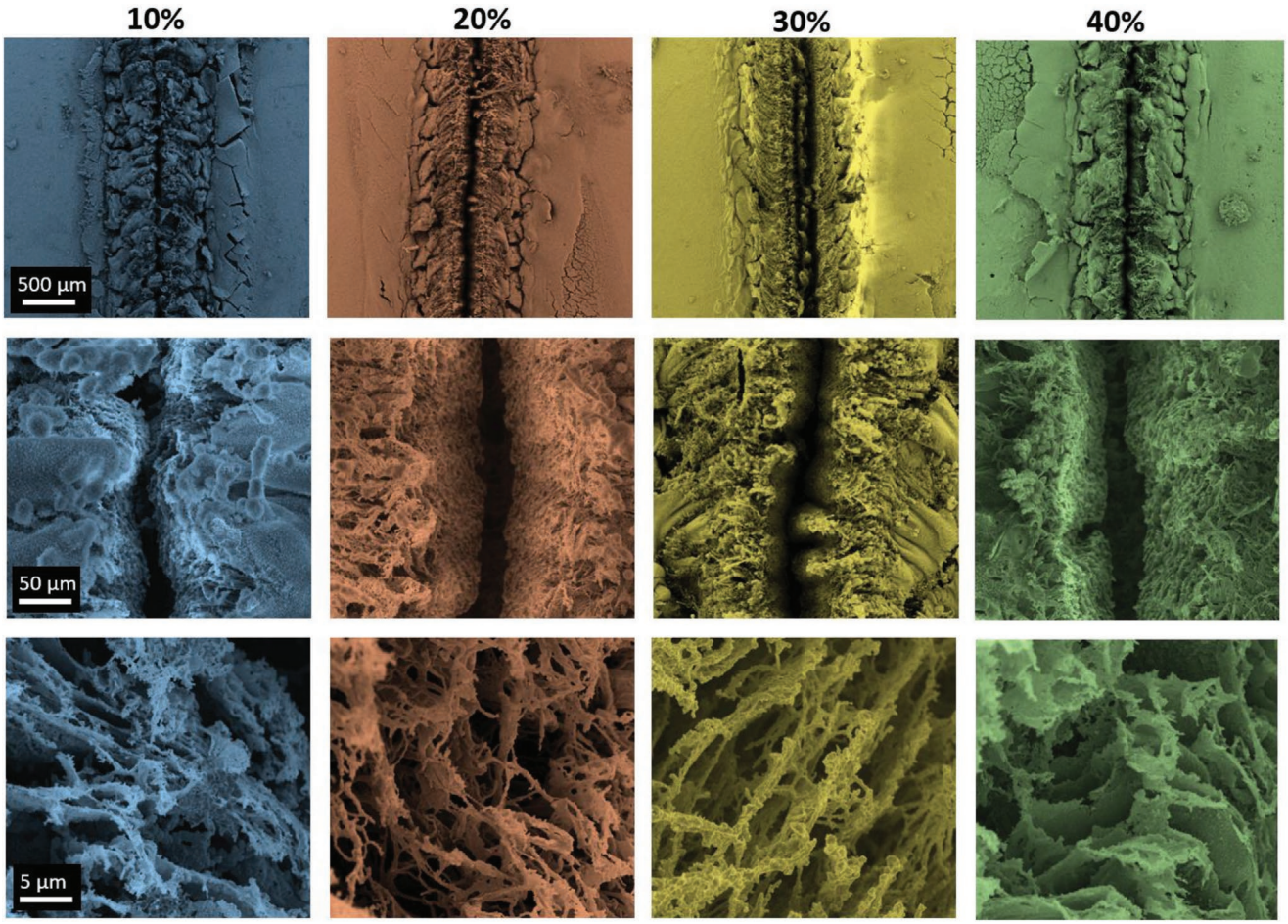

Figure 2. FESEM images at different magnifications (increasing from top to bottom) of the LIG samples obtained from PDMS treated with different concentrations of TEG (10%, 20%, 30%, and 40%).

well known that it is possible to tune the mechanical properties of the PDMS by acting on the crosslinking degree and thus it should be possible to increase the Young's modulus by simply increasing the amount of cross-linking agent with respect to the amount of oligomer.[14]

It is worth noticing that, compared to our previous work,[11] this composite material shows a lower Young's modulus. Indeed, from a starting value of ≈2 MPa the modulus was increased up to 7 MPa in the case of PDMS/polyimide particle composite,[11] and reduced down to a minimum value of 1.02 MPa in the present work.

Figure 2 collects representative FESEM images of the written LIG path starting from PDMS with different concentrations of TEG.

As clearly shown in low-magnification images, the written paths have a different overall morphology with respect to traditional LIG morphology:[12,15] specifically, a distinct hollow region is present right in the middle of the written line, corresponding to the center of the laser beam. This groove is possibly due to a more intense production of gaseous products during the writing process as a consequence of the different composition of the starting polymeric substrate with respect to polyimide, and it has been reported in the literature for PDMS substrates treated with 522 nm laser pulses.[16] This central groove basically divides the LIG path into two distinct parallel lines which exhibit the usual 3D porous morphology, as shown in high-magnification FESEM images. The thin walls of this characteristic 3D architecture are constituted by few-layer graphene flakes, as will be shown in the discussion of TEM results.

Raman spectroscopy gives some insights on the graphenization process of the material. From the plot reported in **Figure 3**, the typical behavior of few-layer graphene is observed after laser treatments, both in pure PDMS and in PDMS treated with TEG. On both spectra, it is possible to identify the D band at ≈1350 cm^{-1}, related to the formation of defects, vacancies and bent sp_2 bonds, the G band at ≈1580 cm^{-1}, originating from a first-order inelastic scattering process involving the degenerate iTO and iLO phonons at the G point (E_{2g} mode) and finally the 2D peak at ≈2700 cm^{-1}, the second harmonic of the D band. A weak signal related with the so-called D′ band at ≈1630 cm^{-1}, still related with material defectiveness, is visible and partially overlapped to the G band. The PDMS treated with laser shows a very intense single-mode 2D peak, with a full width at half maximum of 79 cm^{-1}. This behavior is similar to the one observed in turbostratic graphite, indicating a quite ordered material.[12] Instead, for the TEG-treated material, the intensity of the 2D

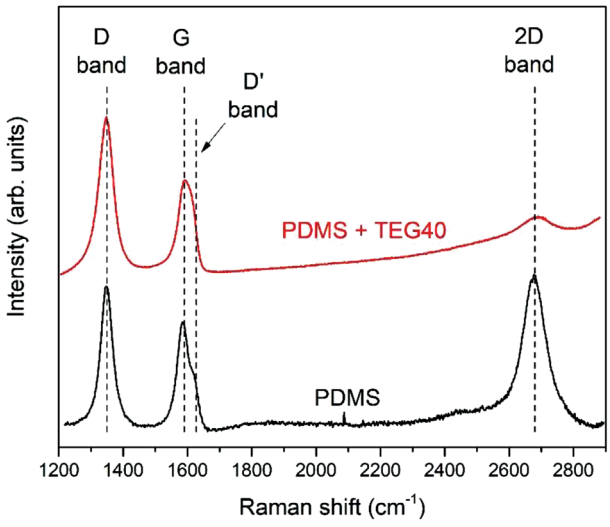

Figure 3. Raman spectra of LIG on PDMS and PDMS with 40% of TEG.

band with respect to the G band is much lower, indicating a lower degree of ordering of the few-layer graphene produced in such case. The I_D/I_G ratio, which can be related with the graphenization degree in the materials,[17] is slightly higher in in PDMS treated with TEG with respect to pure PDMS sample. I_D/I_G values of 1.64 ± 0.16 and 1.33 ± 0.13 are evaluated for PDMS+TEG40 and pure PDMS, respectively.

TEM characterization was implemented in order to achieve a deeper understanding of the graphenic nature of the laser-written path and on the effect of the TEG introduction into the PDMS matrix on the resulting LIG. The main results are reported in **Figure 4** for LIG samples obtained from PDMS and from PDMS treated with 40% TEG. The low-magnification images show representative Bright-Field views of typical fragments of the LIG walls: for both samples, it is interesting to notice the presence of crystalline nanostructures and agglomerates which appear as low-intensity (dark) features due to diffraction contrast and due to their higher average atomic number with respect to the graphenized areas. The analysis of high-resolution images of these particles proves that they are beta-SiC single crystals, as confirmed by Fast Fourier Transforms (FFT)

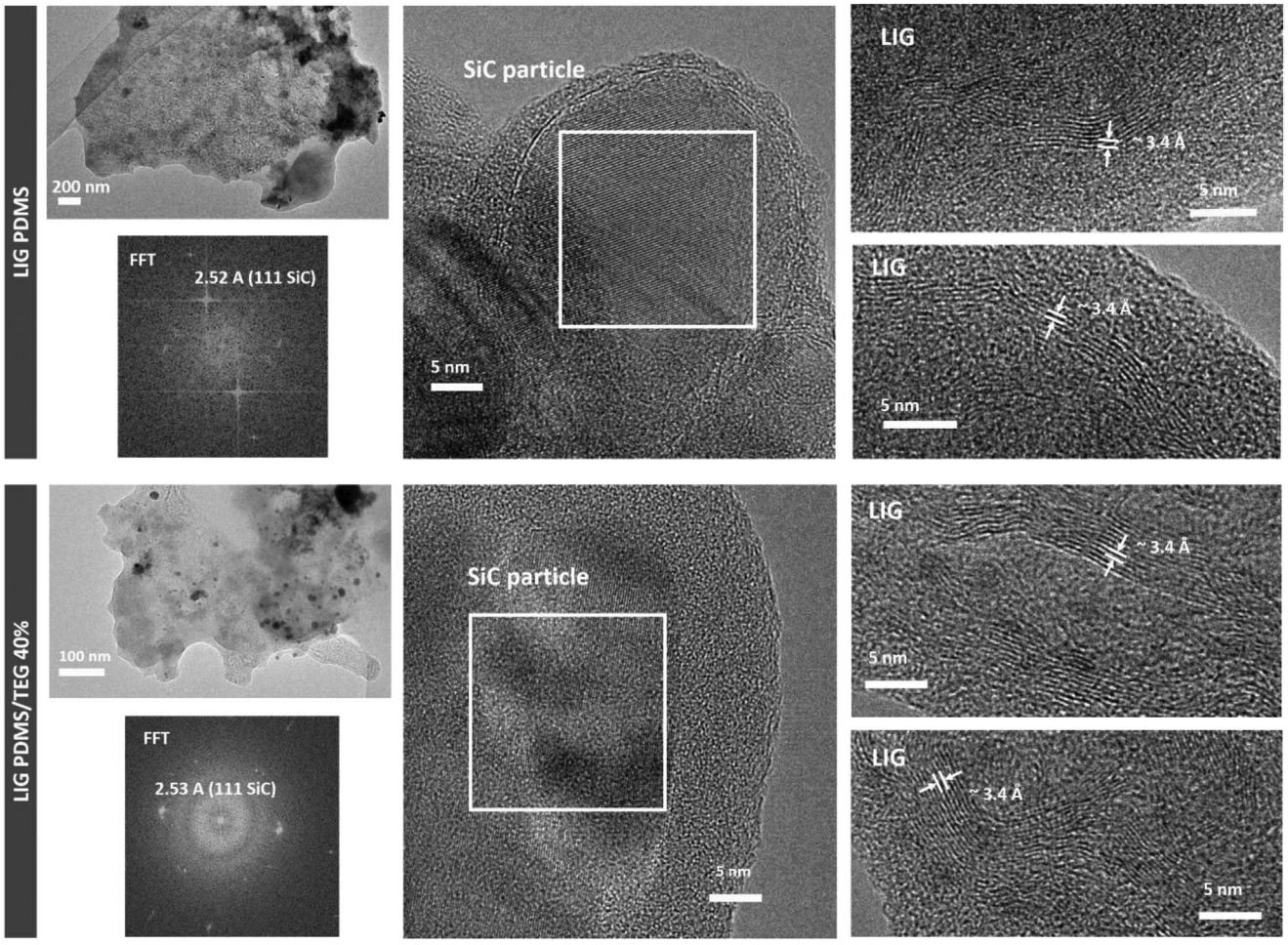

Figure 4. TEM characterization of the LIG samples obtained on PDMS (LIG PDMS) and PDMS treated with 40% TEG (LIG PDMS/TEG 40%). The presented results consist of a low-magnification TEM image (left column) of an LIG region, a high-resolution TEM image of a SiC nanoparticle (central column) with corresponding FFT, high-resolution images of two different regions of the graphenized area (right column).

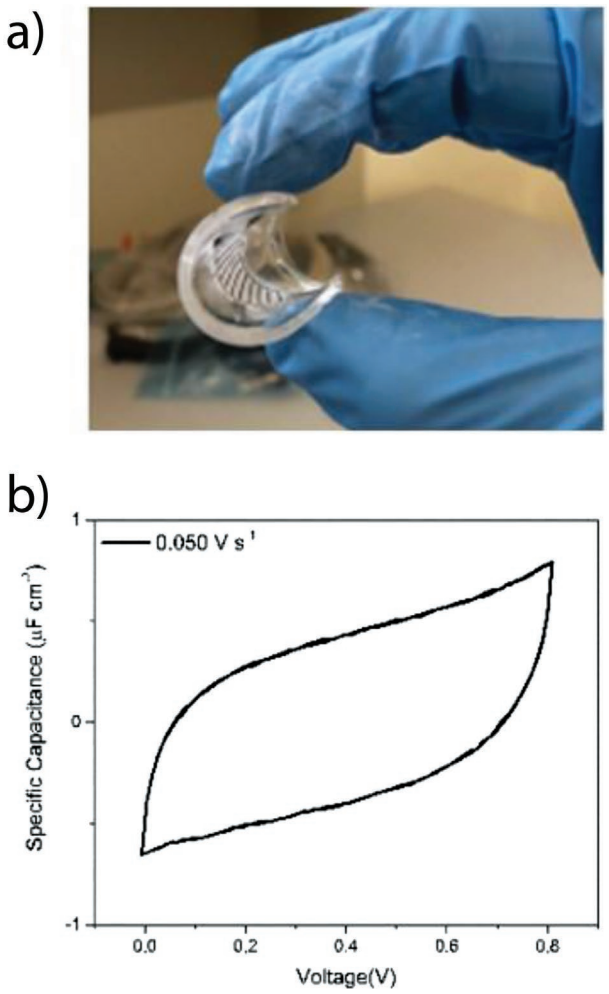

Figure 5. a) Photograph of a supercapacitor obtained on PDMS. b) Voltammogram of the PDMS device recorded at 50 mV s^{-1}.

and by selected area electron diffraction patterns (see the Supporting Information for the details). Qualitatively, it appears that in the LIG PDMS/TEG 40% sample there is a lower density of such nanoparticles with respect to the LIG PDMS sample (see low-magnification images in Figure 4). This is in accordance with the lower abundance of Si atoms in the starting material due to the presence of 40% TEG. The presence of the nanoparticles is not surprising: laser-induced synthesis of SiC nanoparticles from PDMS substrates has already been reported in the literature[16,18] and they are expected to play an important role in the electrical characteristics of the samples, lowering the conductivity of the material. Regarding the graphenized area, for both samples high-resolution TEM images clearly show the presence of a complex structure of randomly oriented few-layer graphene domains, characterized by the ≈3.4 Å *d*-spacing of the (002) family of planes in graphite.

Finally, the best laser parameters were used to write interdigitated LIG pattern onto PDMS substrates with different TEG contents to fabricate microsupercapacitors.

Figure 5 shows the results of the cyclic voltammetry of the bare PDMS converted to LIG at 50 mV s^{-1}. As it can be observed, the typical EDLC shape shows a resistive behavior. In **Figure 6**, we report the voltammograms recorded for the devices with different TEG weight percentage content. All the devices were test at 10, 50, 100, and 500 mV s^{-1} in a potential window of 0.8 V.

CV curves show the typical behavior of EDLC supercapacitors despite the low rate capability. Moreover, as reported in **Figure 7**, by increasing the TEG content it is possible to improve the material specific capacitance as a major carbon density is available for the laser conversion process. We observed that the specific capacitance increases linearly with TEG content, starting from 53 μF cm^{-2} at 10% content up to 297 μF cm^{-2} which is 5,6 times higher and correspond to a 4,6 increase, with respect to the starting capacitance. This trend was confirmed by a linear fit of the obtained discharge capacitances constrained on the intercept value to the one obtained on graphenized PDMS (0.91 μF cm^{-2}), as reported in Figure 7b. In Figure 7a, we show the CDG at 2.5 μA cm^{-2} from which discharge capacitance values were computed.

EIS was used to evaluate, mainly, the transport properties of the devices. As reported in **Figure 8**, it is clear that at all TEG contents the device response reflects an EDLC response. However, the materials' uniformity induces a non-ideal behavior related to high frequency semicircles caused by particle–particle contact resistance. It has not to be excluded a contribution between the silver paste used for contacts and the device LIG pads as a partial contribution to these semicircles.[19] As it can be observed, the overall resistive behavior of the devices decreases with TEG content as well as the amplitude of the semicircles meaning that a more uniform and dense material is being produced. A strange trend is reported concerning the evolution of the imaginary parts, with the blue curve out of trend. However, by moving from 10% up to 40% the imaginary part is also decreasing as evidence of increased device capacitance.

Finally, in **Figure 9** we report the Ragone Plot derived from CV results and compared to the one obtained in a previous work on LIG written on polyimide substrate.[12] As it can be observed, by increasing the amount of carbon material in the PDMS matrix it is possible to tune the energetic performance in a range which is comparable to the standard polyimide technology.

3. Conclusions

In conclusion, we report for the first time the laser graphenization of PDMS, the most commonly used polymer for flexible, stretchable and transparent electronics. By adding TEG into the elastomeric network it is possible to further improve the graphenization step increasing the conductivity of the obtained LIG with monotone dependence on TEG concentration. The addition of the solvent led to the production of a composite material as further proved by IR measurements. Compared to our previous results obtained on PDMS blended with a polyimide powder, the presented substrate material shows different mechanical properties resulting softer. The process was deeply investigated by electron microscopy and Raman measurements, while the electrochemical performance on the obtained conductive paths was evaluated for supercapacitor application. The LIG on PDMS filled with TEG was able to succeed

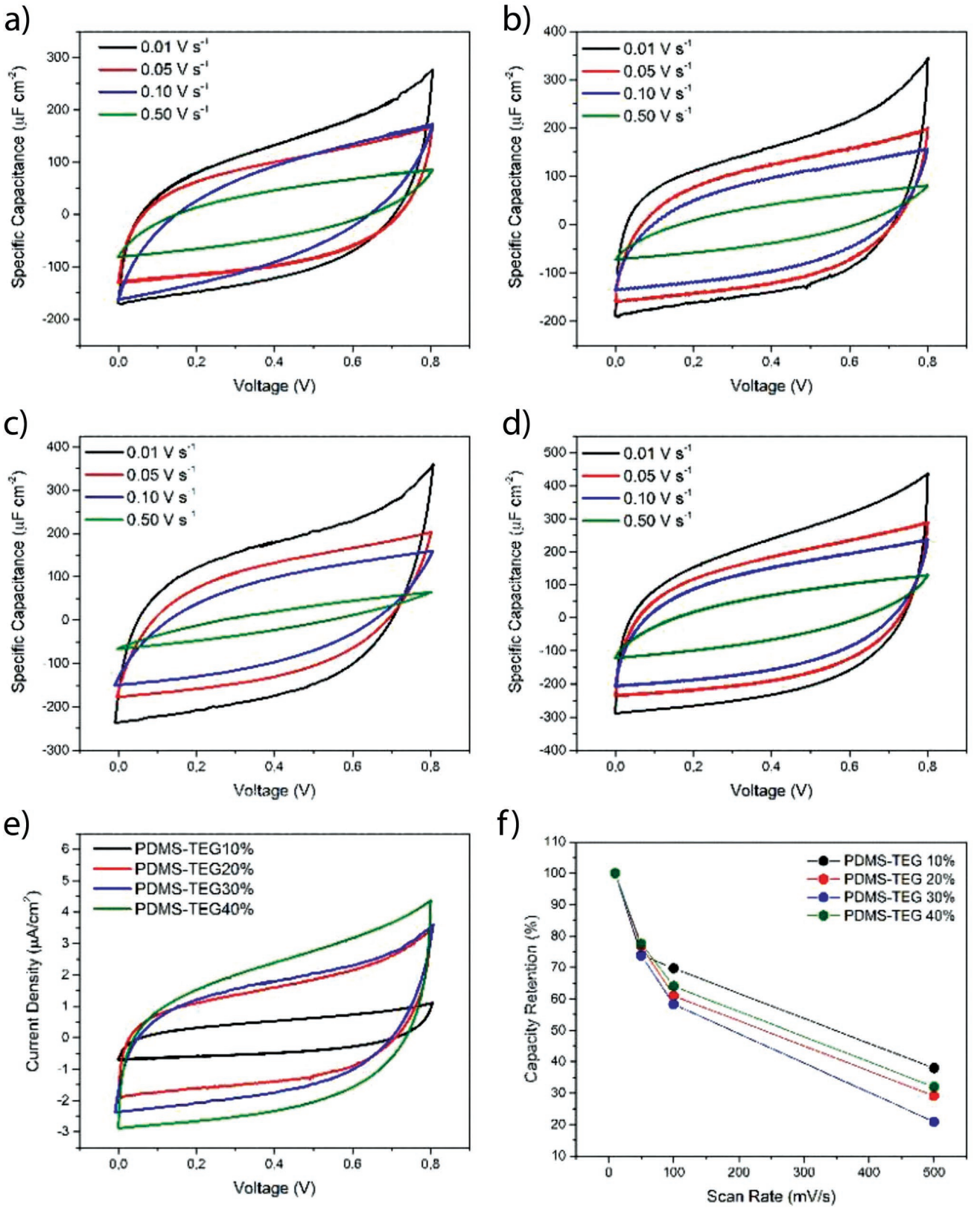

Figure 6. a–d) CV profiles of devices obtained on PDMS-TEG 10%, PDMS-TEG 20%, PDMS-TEG 30%, and PDMS-TEG 40%, respectively, recorded at 10, 50, 100, and 500 mV s^{-1}. e) CVs recorded at 10 mV s^{-1} for different PDMS devices. f) Rate capability rated in the CV experiments.

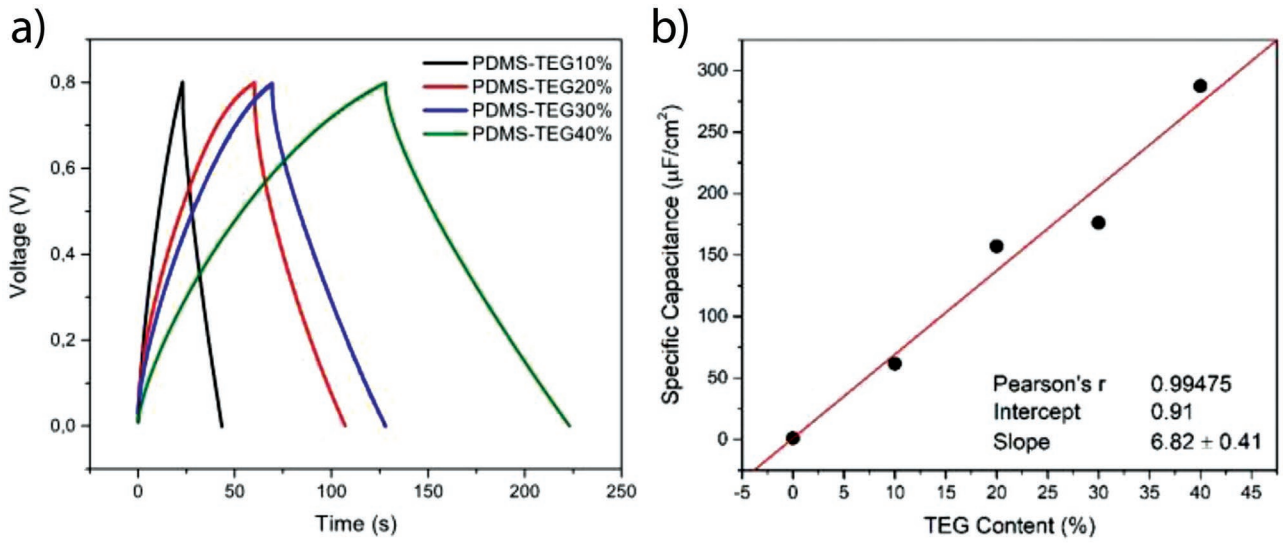

Figure 7. a) CDG measurements carried out at 2.5 μA cm^{-2} on PDMS and PDMS-TEG composites and b) related specific discharge capacitances. It is also reported a linear fit of the obtained values constrained to the 0% result.

energy storage behavior similar to the one achievable using LIG onto polyimide substrate, the most common starting polymer for LIG. The results here presented aim to solve the existing problem about stretchable polymers suitable for flexible supercapacitors fabrication.

4. Experimental Section

Sample Preparation: PDMS prepolymer and curing agent (Sylgard 184, Dow Corning) were manually mixed (mixing ratio 10:1 by weight) and degassed for 1 h. The mixture was poured into a desiccated PMMA mold and then cross-linked at 60 °C for 1 h. Membranes with thickness of 1 mm were removed from the mold and manually cut in 2 × 2 cm^2 pieces. Triethylene glycol (TEG, Sigma Aldrich) was added at different concentrations (10%, 20%, 30%, and 40%) into the PDMS mixture before casting to investigate its effect during laser writing process.

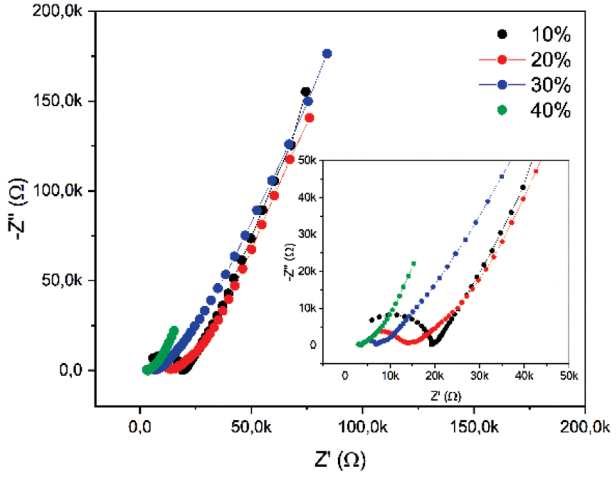

Figure 8. EIS results carried out at 5 mV signal amplitude. At all TEG percentage contents it is possible to appreciate the typical EDLC response with the presence of electrode's parasite interfaces caused by particles interconnections.

Laser Writing: The instrument used for laser writing is an EOX 30 provided by Datalogic, a Pulse Width Modulation (PWM) CO_2 laser with 10 064 nm wavelength. It exploits the use of a galvanometric head in order to address the laser beam, it has two mirrors able to move at a speed ranging from 5 to 6000 mm s^{-1}. The laser is equipped with an autofocus instrument and a hood to absorb the produced vapors. The laser parameters used to control the writing conditions are power and frequency, controlling the duty cycle and period of the PWM signal respectively, the pulse width, defining the number of pulses inside the period, speed, to set the writing speed and finally the number of repetitions.

The power was varied from 1% to 5%, and the frequency was kept at 10 kHz. The writing speed was changed according to the power in order to avoid ablation in the range from 5 to 125 mm s^{-1}. Then the number of repetitions was set to 2.

Materials Characterization: Scanning electron microscopy analysis was performed with a field-emission scanning electron microscope (FESEM Supra 40, Zeiss) equipped with a Si(Li) detector for energy-dispersive X-ray spectroscopy.

TEM characterization was performed with an FEI Tecnai G2 F20 S-TWIN microscope operated at 200 kV acceleration voltage. Concerning sample preparation, portions of the LIG PDMS and LIG PDMS/TEG 40% samples were detached by brief sonication into high purity ethanol and subsequently drop-casted to holey-carbon TEM grids.

The analysis of TEM images was performed with Gatan Microscopy Suite (GMS) software; the analysis of electron diffraction patterns was carried out using the Circular Hough transform diffraction analysis tool.[17]

Raman characterization was performed by means of a Renishaw InVia micro-Raman spectrometer, equipped with a cooled CCD camera. A laser diode source (λ = 514.5 nm) was used with 5 mW power, and sample inspection occurred through a microscope objective (50×), with a backscattering light collection setup.

X-Ray Diffraction measurements (Panalytical X'Pert MRD Pro X-ray diffractometer with a Cu Kα source) were used to investigate the presence of SiC in the laser-treated samples. The measurements were performed with a scan speed of 200 s per step and a step size of 0.026° in Brag–Brentano configuration.

The mechanical properties of the PDMS and PDMS/TEG composite samples were evaluated with a Universal Testing System (Instron 3365). All the samples were prepared by casting slice of 40 mm length, 5 mm width, and 1 mm thickness.

Fourier transformed infrared (FTIR) spectra were recorded using a Nicolet 5700 FTIR Spectrometer used in attenuated total reflectance (ATR) mode with 2 cm^{-1} resolution and an average of 32 scans.

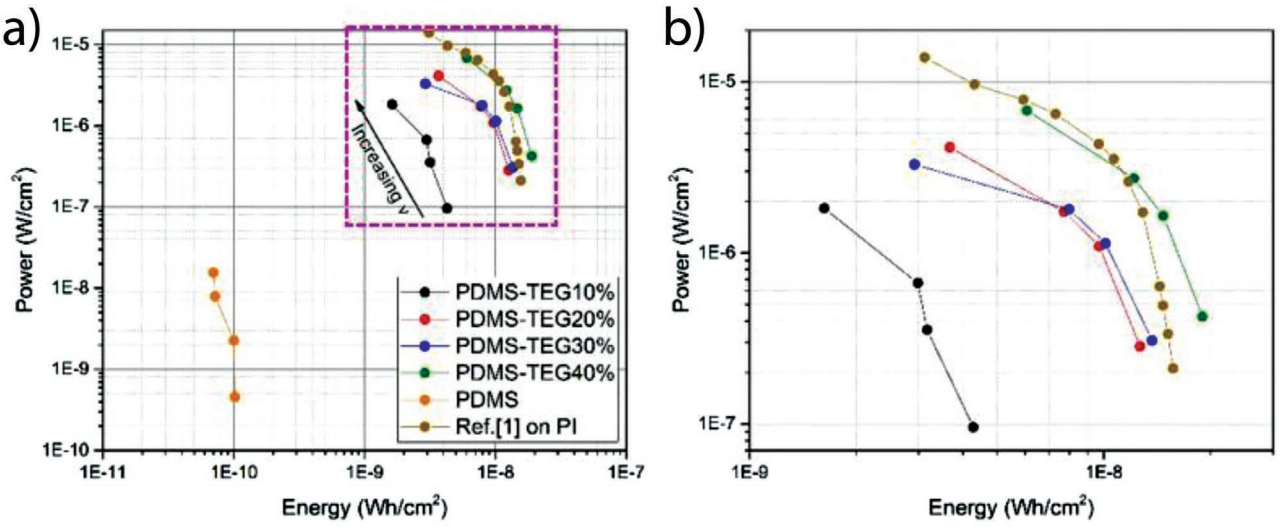

Figure 9. a) Ragone plot derived by the cyclic voltammetry analyses on PDMS and PDMS-TEG composites compared to the work of ref. [12] on polyimide substrate. b) A zoom on the high energy–high power region.

Static contact angle (CA) measurements were performed using OCA H200 Dataphysics equipment in ambient conditions. The sessile drop method was implemented employing water droplets with 1 µL volume. Results of both FTIR and CA are collected in the supporting information.

Electrochemical characterizations were run with Metrohm Autolab Equipped with M101 potentiostat–galvanostat module and FRA32M for Electrochemical Impedance Spectroscopy. Some measurements were run in a Faraday cage in order to suppress the noise contribution for very low currents measurement both in potentiostatic and galvanostatic operation modes.

Cyclic voltammetries were run in a potential window of 0.8 V at 10, 50, 100, and 500 mV s^{-1}, while galvanostatic charge and discharge measurements (CDG) were performed according to devices rate capabilities spanning from 0.2 µA cm^{-2} for pure PDMS devices up to 25 µA cm^{-2} for the 40% TEG ones. However, for the composite-based devices at least one current rate is chosen to make a galvanostatic comparison, and that rate being 2.5 µA cm^{-2}.

Devices were contacted by applying silver paste, for such a reason they could not be immersed in any electrolyte, thus the ionic contact was made thanks to paper-based separator swelled with 1 M Na_2SO_4.

Supporting Information

Supporting Information is available from the Wiley Online Library or from the author.

Acknowledgements

This result is part of a project that has received funding from the European Research Council (ERC) under the European Union's ERC Starting Grant CO_2CAP Grant agreement No. 949916 (Energy harvesting from CO_2 emission exploiting ionic liquid-based CAPacitive mixing).

Open Access Funding provided by Politecnico di Torino within the CRUI-CARE Agreement.

Conflict of Interest

The authors declare no conflict of interest.

Data Availability Statement

Research data are not shared.

Keywords

flexible devices, laser-induced graphene, LIG, PDMS, supercapacitors

Received: June 22, 2021
Revised: October 5, 2021
Published online: November 10, 2021

[1] a) Z. Bao, X. Chen, *Adv. Mater.* **2016**, *28*, 4177; b) J. K. Chang, H. P. Chang, Q. Guo, J. Koo, C. I. Wu, J. A. Rogers, *Adv. Mater.* **2018**, *30*, 1704955; c) C. Wang, K. Xia, H. Wang, X. Liang, Z. Yin, Y. Zhang, *Adv. Mater.* **2019**, *31*, 1801072.

[2] a) Y. Zhan, Y. Mei, L. Zheng, *J. Mater. Chem. C* **2014**, *2*, 1220; b) S. T. Han, H. Peng, Q. Sun, S. Venkatesh, K. S. Chung, S. C. Lau, Y. Zhou, V. A. L. Roy, *Adv. Mater.* **2017**, *29*, 1700375; c) P. Yang, J. Xie, L. Wang, X. Chen, F. Wu, Y. Huang, *Adv. Mater. Interfaces* **2020**, *7*, 2070100.

[3] I. Lee, K. Lee, *Bus. Horizons* **2015**, *58*, 431.

[4] K. D. Harris, A. L. Elias, H. J. Chung, *J. Mater. Sci.* **2016**, *51*, 2771.

[5] a) T. Liu, L. Zhang, B. Cheng, X. Hu, J. Yu, *Cell Rep. Phys. Sci.* **2020**, *1*, 100215; b) X. Huang, Z. Yin, S. Wu, X. Qi, Q. He, Q. Zhang, Q. Yan, F. Boey, H. Zhang, *Small* **2011**, *7*, 1876.

[6] R. Ye, D. K. James, J. M. Tour, *Acc. Chem. Res.* **2018**, *51*, 1609.

[7] Y. Chyan, R. Ye, Y. Li, S. P. Singh, C. J. Arnusch, J. M. Tour, *ACS Nano* **2018**, *12*, 2176.

[8] a) M. P. Wolf, G. B. Salieb-Beugelaar, P. Hunziker, *Prog. Polym. Sci.* **2018**, *83*, 97; b) A. Lamberti, S. L. Marasso, M. Cocuzza, *RSC Adv.* **2014**, *4*, 61415; c) A. Larmagnac, S. Eggenberger, H. Janossy, J. Vörös, *Sci. Rep.* **2014**, *4*, 7254; d) A. Lamberti, *Appl. Surf. Sci.* **2015**, *335*, 50; e) A. Lamberti, A. Virga, P. Rivolo, A. Angelini, F. Giorgis, *J. Phys. Chem. B* **2015**, *119*, 8194; f) L. Pasquardini, C. Potrich, M. Quaglio, A. Lamberti, S. Guastella, L. Lunelli, M. Cocuzza, L. Vanzetti, C. F. Pirri, C. Pederzolli, *Lab Chip* **2011**,

11, 4029; g) A. Lamberti, A. Angelini, S. Ricciardi, F. Frascella, *Lab Chip* **2015**, *15*, 67.

[9] a) W. Song, J. Zhu, B. Gan, S. Zhao, H. Wang, C. Li, J. Wang, *Small* **2018**, *14*, 1703321; b) R. Rahimi, M. Ochoa, W. Yu, B. Ziaie, *ACS Appl. Mater. Interfaces* **2015**, *7*, 4463.

[10] A. Lamberti, F. Clerici, M. Fontana, L. Scaltrito, *Adv. Energy Mater.* **2016**, *6*, 1600050.

[11] M. Parmeggiani, P. Zaccagnini, S. Stassi, M. Fontana, S. Bianco, C. Nicosia, C. F. Pirri, A. Lamberti, *ACS Appl. Mater. Interfaces* **2019**, *11*, 33221.

[12] A. Lamberti, F. Perrucci, M. Caprioli, M. Serrapede, M. Fontana, S. Bianco, S. Ferrero, E. Tresso, *Nanotechnology* **2017**, *28*, 174002.

[13] J. Lin, Z. Peng, Y. Liu, F. Ruiz-Zepeda, R. Ye, E. L. G. Samuel, M. J. Yacaman, B. I. Yakobson, J. M. Tour, *Nat. Commun.* **2014**, *5*, 5714.

[14] A. Lamberti, M. Di Donato, A. Chiappone, F. Giorgis, G. Canavese, *Smart Mater. Struct.* **2014**, *23*, 105001.

[15] R. Ye, D. K. James, J. M. Tour, *Adv. Mater.* **2019**, *31*, 1803621.

[16] S. Hayashi, F. Morosawa, M. Terakawa, *Nanoscale Adv.* **2020**, *2*, 1886.

[17] D. R. G. Mitchell, *Ultramicroscopy* **2008**, *108*, 367.

[18] Y. Nakajima, S. Hayashi, A. Katayama, N. Nedyalkov, M. Terakawa, *Nanomaterials* **2018**, *8*, 558.

[19] S. Dsoke, X. Tian, C. Täubert, S. Schlüter, M. Wohlfahrt-Mehrens, *J. Power Sources* **2013**, *238*, 422.